Flux dynamics associated with the second magnetization peak in the iron pnictide $Ba_{1-x}K_xFe_2As_2$

S. Salem-Sugui, Jr.,[1] L. Ghivelder,[1] A. D. Alvarenga,[2] L. F. Cohen,[3] K. A. Yates,[3] K. Morrison,[3] J. L. Pimentel, Jr.,[4] Huiqian Luo,[5] Zhaosheng Wang,[5] and Hai-Hu Wen[5]

[1]*Instituto de Fisica, Universidade Federal do Rio de Janeiro, 21941-972 Rio de Janeiro, RJ, Brazil*

[2]*Instituto Nacional de Metrologia Normalização e Qualidade Industrial, 25250-020 Duque de Caxias, RJ, Brazil*

[3]*The Blackett Laboratory, Physics Department, Imperial College London, London SW7 2AZ, United Kingdom*

[4]*Instituto de Fisica, Universidade Federal do Rio Grande do Sul, Porto Alegre, RS, Brazil*

[5]*National Laboratory for Superconductivity, Institute of Physics and National Laboratory for Condensed Matter Physics, P.O. Box 603, Beijing 100190, People's Republic of China*

(Received 9 March 2010; revised manuscript received 23 July 2010; published 12 August 2010)

We report on isofield magnetic relaxation data on a single crystal of $Ba_{1-x}K_xFe_2As_2$ with superconducting transition temperature $T_c=32.7$ K which exhibit the so-called fish-tail effect. A surface map of the superconducting transition temperature shows that the superconducting properties are close to homogeneous across the sample. Magnetic relaxation data, $M(t)$, was used to obtain the activation energy $U(M)$ in order to study different vortex-dynamics regimes. Results of this analysis along with time-dependent measurements as a function of field and temperature extended to the reversible region of some $M(H)$ curves demonstrate that the irreversibility as well the second magnetization peak position, $H_p(T)$, are time dependent and controlled by plastic motion of the vortex state. In the region delimited by a characteristic field Hon (well below H_p), and H_p, the vortex dynamics is controlled by collective pinning. For fields below Hon the activation energy, U_0, increases with field as expected for collective pinning, but the pinning mechanism is likely to be in the single vortex limit.

DOI: 10.1103/PhysRevB.82.054513 PACS number(s): 74.25.Uv, 74.25.Wx, 74.25.Sv, 74.70.Xa

I. INTRODUCTION

The recent discovery of the iron-pnictides superconductor systems[1–3] with critical temperatures ranging from 20 to 55 K raised an intense interest on the study of their properties, such as pairing mechanism, themodynamics and transport, normal-state band structure, etc. Among these works, one can also find few studies dedicated to the vortex dynamics, which due to their relatively high T_c and upper critical field H_{c2}, are gaining interest for applications. Iron-pnictides materials, depending on each system and doping, exhibit the peak effect in the critical current, which is associated with a second magnetization peak appearing in the magnetization field $M(H)$ curves. Some of these systems also present a large magnetic relaxation which resembles, for instance, the giant magnetic relaxation observed in the cuprates.[4] The study of the second magnetization peak also known as the "fish-tail" peak is of great interest, from both, academic as well technological view points.[5,6] Fundamentally speaking, the mechanism and the origin of this effect is still much debated partly because it is system dependent with classification predominantly determined by superconducting anisotropy.[5–10]

So far, flux-dynamics studies of the second magnetization peak in iron pnictides were performed on the systems, $SmFeAsO_{0.9}F_{0.1}$ with $T_c=55$ K where the authors inferred weak and collective pinning,[11] $NdFeAsO_{0.85}$ (Ref. 12) and $Ba(Fe_{1-x}Co_x)_2As_2$, the most studied system, where the peak effect appears only for samples near optimally doping[13–18] and weak and collective pinning are claimed in most of the works. The fish tail has been also observed in $Ba_{0.6}K_{0.4}Fe_2As_2$ with $T_c=36.5$ K and studied from transport measurements.[19] It is interesting to mention that the slightly underdoped samples of the $Ba_{1-x}K_xFe_2As_2$ system ($T_c \gtrsim 30$ K) presents a phase-separated coexistence of antiferromagnetism and superconductivity[20] which might be associated to the fact that samples with T_c below 28 K do not show the second magnetization peak. Indeed it is likely that most forms of inhomogeneity (T_c variation, doping variation, impurity phases, and magnetic inclusions) will wash out the peak effect. Its observation is usually related to sample purity. Studies on $Ba(Fe_{1-x}Co_x)_2As_2$ includes; determination of the normalized flux-pinning force around the second magnetization peak;[15] collective to plastic pinning crossover at the peak suggested by flux-creep data and relaxation rate analysis;[16] collective to plastic pinning crossover at the peak inferred by flux-creep data and the generalized-inversion-scheme analysis for the activation energy;[13] fish tail studied by magnetic measurements and magneto-optical imaging;[14] observation of a highly disordered vortex state from Bitter decoration and small-angle neutron scattering;[17] vortex-state structural phase transition at the peak from magnetization and flux-creep measurements within a thermodynamics analysis.[18] The above studies are summarized in Table I below with comments of the type of measurement performed and the main conclusions of the study.

Importantly, the possibility that a first-order phase transition instead of a vortex-dynamics crossover has been proposed to explain the second magnetization peak in the pnictides demonstrates the need of more detailed and rigorous vortex-dynamics analysis. It is that motivated the present work. Another point not covered in the literature is the study of the crossover that should exist at the onset field of the fish tail, also known as *Hon*. Phenomenologically speaking one should expect a crossover from single to collective pinning at Hon because magnetization changes curvature at Hon, and it appears that this matter has not been studied in detail. In this

TABLE I. Iron-pnictide systems which show the fish-tail effect.

Studied samples	T_c	Measurements+results	Conclusions
$NdFeAsO_{0.85}$ polycrystalline-Moore *et al.*, Ref. 12	T_c=46 K	Fish tail associated to a maximum in the creep rate with field at T=20,35 K	
$SmFeAsO_{0.9}F_{0.1}$ polycrystalline Yang *et al.*, Ref. 11	T_c=55 K	$M(H)$ curves-dynamic and traditional creep rates+activation energy analysis	Weak collective pinning
$BaFe_{(1-x)}Co_xAs_2$ single crystal Nakajima *et al.*, Ref. 14	$T_c\sim$25 K	$M(H)$ curves-Bean-type penetration of vortices by magneto-optical images	
$BaFe_{0.9}Co_{0.1}As_2$ single crystal Yamamoto *et al.*, Ref. 15	T_c=22 K	$M(H)$ curves-normalized pinning force scaling independent of T around second peak	Dominant strong vortex pinning mechanism
$BaFe_{0.93}Co_{0.07}As_2$ single crystal Eskildsen *et al.*, Ref. 17	T_c=22 K	Low-field Bitter decoration+small-angle neutron scattering	High-disordered vortex-state due to strong pinning. Absence of collective pinning
$BaFe_{0.926}Co_{0.074}As_2$ single crystal Prozorov *et al.*, Ref. 16	T_c=22 K	$M(H)$ curves-creep rate around second peak-Activation-energy comparison-	Collective pinning $H<H_p$ Plastic pinning $H>H_p$
$BaFe_{(1-x)}Co_xAs_2$ single crystals samples as a function of x Shen *et al.*, Ref. 13	Fish tail $x\sim$0.08 $T_c\sim$20–25 K	$M(H)$ curves-dynamic creep rate around second peak-Generalized inversion scheme for activation energy-	Collective to plastic for $H>H_p$ Collective pinning $H<H_p$
$BaFe_{0.925}Co_{0.025}As_2$ single crystal Kopeliansky *et al.*, Ref. 18	T_c=25 K	$M(H)$ curves-creep rate around second peak as function of T thermodynamics analysis	Phase transition of the vortex state near H_p
$Ba_{0.6}K_{0.4}Fe_2As_2$ single crystal Yang *et al.*, Ref. 19	T_c=36 K	$M(H)$ curves-vortex pinning force around second peak	Pinning by small-size normal cores
This work $Ba_{(1-x)}K_xFe_2As_2$ $x\sim$0.28 single crystal	T_c=32.7 K	T_c Map+$M(H)$ curves+magnetic relaxation from $H<$Hon up to $H>H_p$-smooth activation-energy curves obtention+creep Rate analysis	Collective to plastic at H_p-single to collective at Hon without change in the creep rate behavior

work we address these above points by performing a detailed study of the vortex dynamics as a function of magnetic field and temperature in an iron pinictide single crystal of $Ba_{1-x}K_xFe_2As_2$ with superconducting transition temperature T_c=32.7 K which exhibits the fish-tail effect. The work addresses the existence of a change in the pinning mechanism (or crossover) associated with the anomalous second magnetization peak, as found in YBaCuO (Ref. 21) and the pinning crossover expected to exist at Hon. This work complements a previous study of the vortex-phase diagram performed on the same system[19] and as above-mentioned vortex-dynamics studies performed in other pinictides systems[11,13,14,16] using different approaches. The experiment is conducted by obtaining magnetic relaxation data over selected isothermic M vs H curves, $M(H)$, for magnetic fields values ranging from just above H_{c1} [actually above the first penetration field peak appearing in isothermic magnetization $M(H)$ curves] up to field values close to the irreversible point Hirr. Magnetic relaxation curves are used to obtain the corresponding activation energies[22] allowing the study of the pinning mechanism for magnetic fields in the region of the anomalous second peak as treated in Ref. 21 and below the field Hon. We have also measured isofield zero-field-cooled magnetization curves as a function of temperature, M vs T curves. All data, $M(H)$ and M vs T curves, were obtained for $H\|c$ axis. The M vs T curves were used to obtain the near equilibrium irreversibility line, since $M(H)$ curves obtained at different effective dH/dt rates shown that the irreversible point is time dependent.

Results of this work show that the temperature dependence of the second magnetization peak position, H_p and of the irreversibility field Hirr are well explained in terms of a plastic motion of the vortex lattice. Results also demonstrate the existence of a crossover in the pinning mechanism at Hon, where apparently, this crossover occurs without a change in the behavior of the activation energy U_0 with field (increasing with field).

II. EXPERIMENTAL

We measure a high-quality crystal of $Ba_{1-x}K_xFe_2As_2$ with T_c=32.7 K corresponding to a potassium content x=0.28 and with mass of approximately 0.05 mg. This is the same sample studied in our previous work[23] and show a fully de-

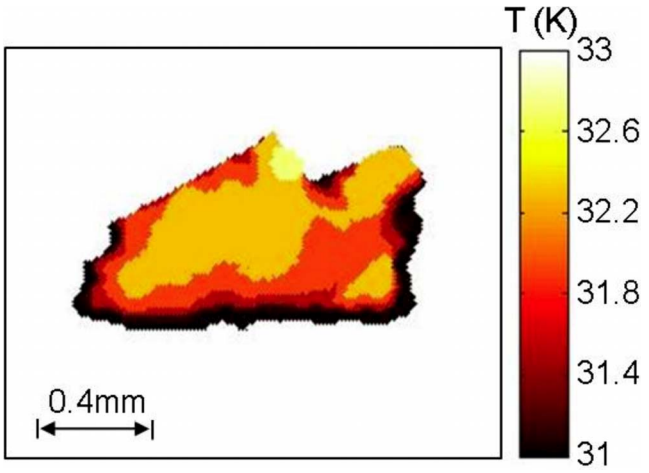

FIG. 1. (Color online) Surface map of the superconducting transition temperature of the studied sample. The transition temperatures of the scanned surface are identified by colors labeled on the right.

veloped superconducting transition with width $\Delta T_c \simeq 1$ K. The crystal was grown by a flux method described elsewhere.[3] Magnetization and magnetic relaxation data were taken after cooling the sample in zero applied magnetic field (but in the presence of the earth magnetic field). A commercial magnetometer, based on a superconducting quantum interference device was used for bulk magnetization measurements and a scanning Hall probe magnetometer[24] was used to map the superconducting transition temperature distribution over the entire sample and to obtain few isothermal images of magnetic field profile in the sample with a spatial resolution of 5 μm. Magnetization vs field, $M(H)$ curves

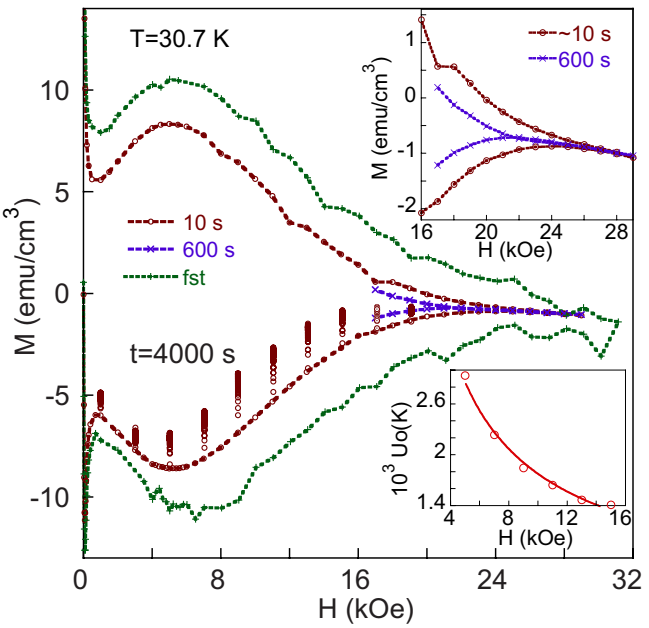

FIG. 2. (Color online) Isothermic $M(H)$ curves at $T=30.7$ K plotted with $M(t)$ data obtained for fixed fields. The upper inset show detail of data for fields near the reversible region. The lower inset shows a plot of U_{0pl} vs H for $H \gtrsim H_p$.

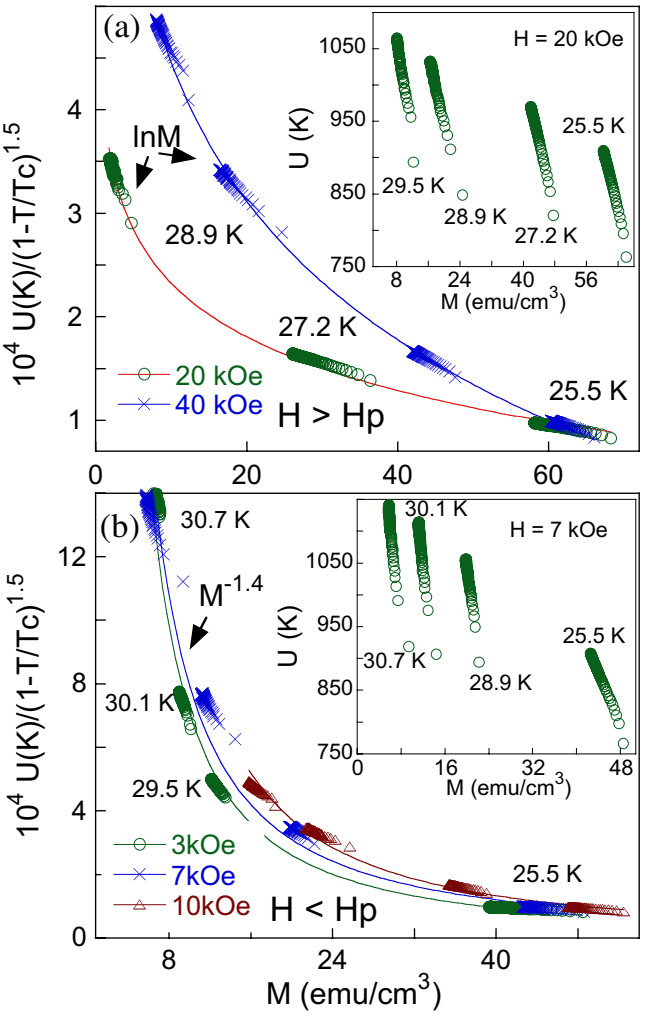

FIG. 3. (Color online) Activation energy $U(M,T)$ for fixed fields after scaled by the scaling function $g(T/T_c)=(1-T/T_c)^{1.5}$; (a) for fields $H \gtrsim H_p$; (b) for fields Hon $\lesssim H \lesssim H_p$. Insets show $U(t)$ vs M curves for selected fields prior scaling.

were obtained at fixed temperatures ranging from 24 to 32 K, for fields up to 50 kOe. All $M(H)$ curves were obtained by extracting the data after the field was stabilized, in most cases the superconducting magnet was set in persistent mode. Additional curves were obtained with the magnet in the nonpersistent (driven) mode, in order to obtain the hysteresis curves. Magnetic relaxation data, $M(t)$ curves, were obtained at $\simeq$60 s intervals over a period of $\simeq$4000 s for fields in the lower branch (increasing field) of selected isothermic hysteresis curves. We also measure long-time magnetic relaxation curves over a period of 12 h for selected values of magnetic field at $T=29.5$ and 28.9 K. Few magnetic relaxation data were measured on the upper branch (decreasing field) of the hysteresis curves to check for data symmetry, which confirm that bulk pinning is dominant for the studied isothermals. We also obtained isofield zero-field-cooled and field-cooled magnetization curves, M vs T, with fields ranging from 0.05 to 30 kOe.

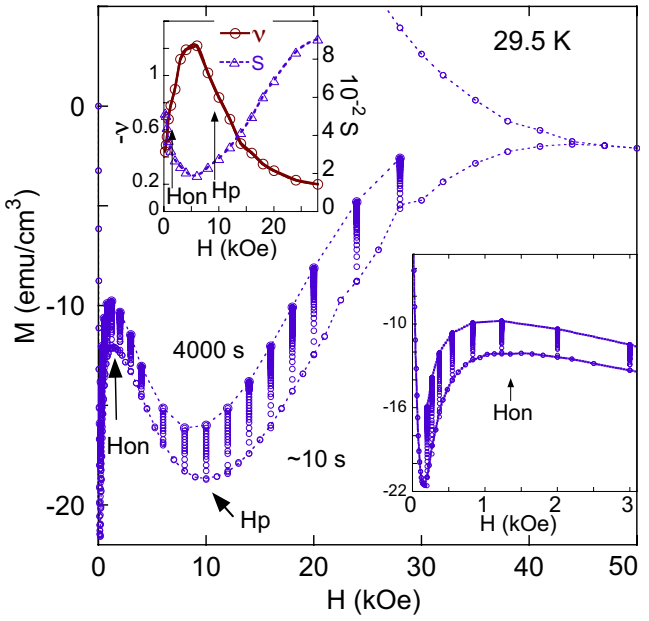

FIG. 4. (Color online) Isothermic $M(H)$ curves at $T=29.5$ K plotted with $M(t)$ data obtained for fixed fields. The lower inset shows detail of data for low fields. The upper inset show a double plot of the exponent ν vs H (left y axis) and $S=(1/M_0)dM/d\ln t$ vs H (right y axis).

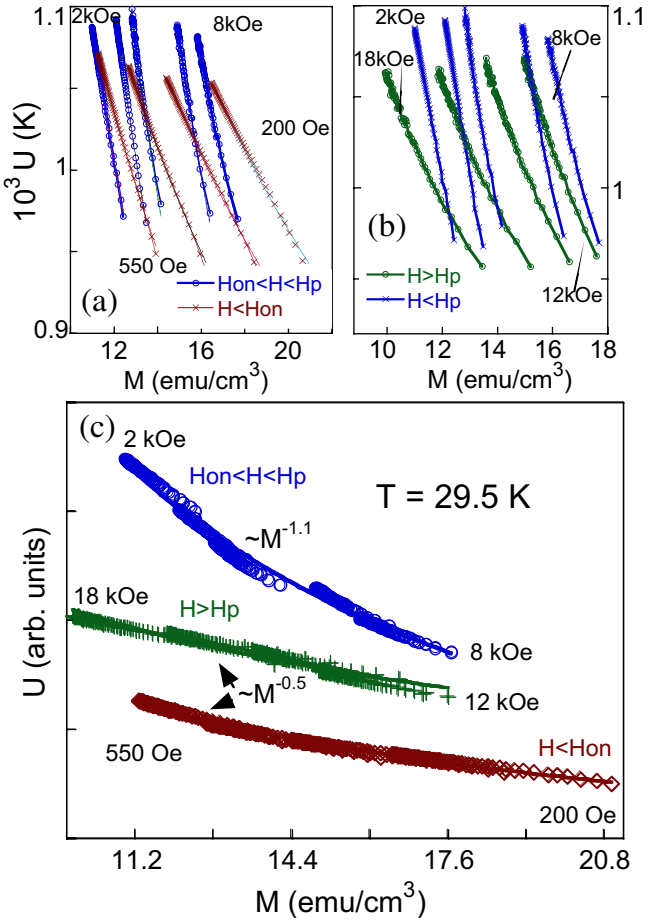

FIG. 5. (Color online) $U(M)$ curves as obtained from $M(t)$ curves at 29.5 K: (a) $U(M)$ curves for fields $H \lesssim$ Hon and Hon $\lesssim H \lesssim H_p$; (b) $U(M)$ curves for fields Hon $\lesssim H \lesssim H_p$ and $H \gtrsim H_p$; and (c) $U(M)$ curves after scaled.

III. RESULTS AND DISCUSSION

Figure 1 shows a surface map of the superconducting transition temperature T_c as obtained from the scanning Hall probe magnetometer with a 0.1 kOe field applied parallel to the c axis after a zero-field-cooled procedure. It is possible to see from Fig. 1 that the sample is basically formed by two major regions, corresponding to more than 90% of the sample, one with $T_c=31.8$ K that surrounds an inner region, the larger one with $T_c=32.3$ K. The sample also has a very small border or edge region with $T_c=31.2$ K corresponding to about 5% of the sample, and an even smaller region with T_c 32.8 K. The T_c homogeneity of the sample can be considered in very good approximation to be within 0.5 K, showing that the sample is of high quality and any effect due to sample inhomogeneity is expected to be negligible.

Figure 2 shows typical magnetization curves, $M(H)$, obtained at $T=30.7$ K exhibiting the anomalous second magnetization peak. Most of the $M(H)$ curves obtained in this work show the fish tail as depicted in Fig. 2, allowing the extraction of the values of the fields Hon, the field above which the second peak is formed, H_p, the field which marks the second peak position, and Hirr which marks the field above which magnetization is reversible. The detail shown by plotting different curves on Fig. 2 is the time dependence of magnetization. The outer curve of Fig. 1 was obtained in the fastest way allowed by the equipment with an effective field sweep rate of ≈50 Oe/s while the internal curve is obtained with an effective field rate of ≈1.5 Oe/s. The third curve was obtained near the irreversibility region with a delay time of 10 min after each field value is stabilized. The large difference between these three $M(H)$ curves evidences the large magnetic relaxation of this system as reported elsewhere. The upper inset of Fig. 2 shows in detail the relaxation effect on the irreversible field Hirr. It is possible to see from Fig. 2 that both, H_p and Hirr are time dependent and that their values drop with time. Similar $M(H)$ curves with 10 min time delay as in Fig. 2 were also obtained at $T=30.1$ and 31.3 K

Figure 2 also shows magnetic relaxation data measured during 4000 s for selected fields around the second magnetization peak which are plotted with the original $M(H)$ curve. Magnetic relaxation curves, $M(t)$, as show in Fig. 2 allow to study the vortex dynamics and have been obtained on six isothermic $M(H)$ curves for fields going from below Hon to above H_p. Magnetic relaxation curves, $M(t)$, were collected for a set of selected magnetic fields on M vs H curves at $T=25.5$, 27.2, 28.9, 29.5, 30.1, and 30.7 K. All M vs $\log(t)$ curves obtained during 4000 s follow the typical linear curve observed in most flux creep experiments. This trend was also observed for 12 h relaxation data obtained for fields above Hon but not for fields below Hon, as will be discussed later.

We analyzed flux-creep data by following one of two different approaches. Either we obtained the relaxation rate $S=(1/M_0)dM(t)/d\ln t$ for each $M(t)$ curve and analyzed its behavior with H (Refs. 25–27) or we analyze the activation energy $U(M)$ by fitting each curve to the expression pre-

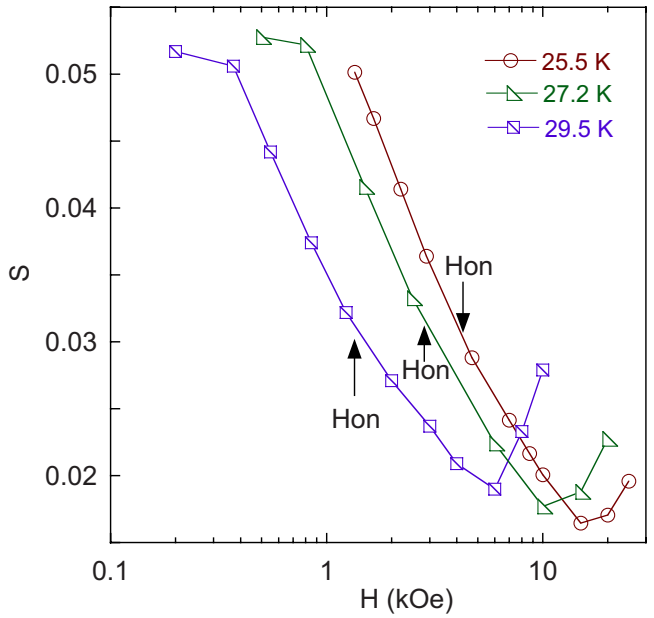

FIG. 6. (Color online) The relaxation rate S is plotted against the magnetic field in logarithmic scale for selected temperatures. The plot displays values of S as obtained for fields below Hon up to fields close to H_p.

dicted by the collective pinning theory, $U(H,M) = U_0(H)[M(t)/M_0]^{\nu}$, which allow to study the behavior of the exponent ν with H. In the last expression $M(t)$ replaces $M(t)$-M_{eq}, where M_{eq} is the equilibrium magnetization, obtained from the average magnetization of both branches in each $M(H)$ curve.

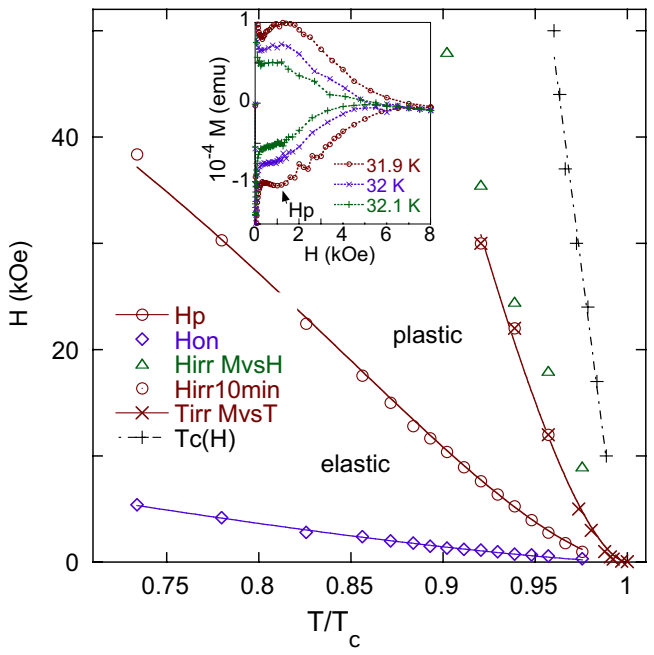

FIG. 7. (Color online) Vortex phase diagram of the studied sample. Solid lines on Tirr(T) and $H_p(T)$ data were obtained by fitting the respective data to the expression $\approx[1-(T/T_c)^4]^{1.7}$, solid line on Hon($T$) data was obtained by fitting the data to the expression $\approx(1-T/T_c)^{1.35}$, while dotted line on $T_c(H)$ data is only a guide to the eyes. The inset show $M(H)$ curves obtained near T_c detailing the temperature onset of the anomalous second magnetization peak.

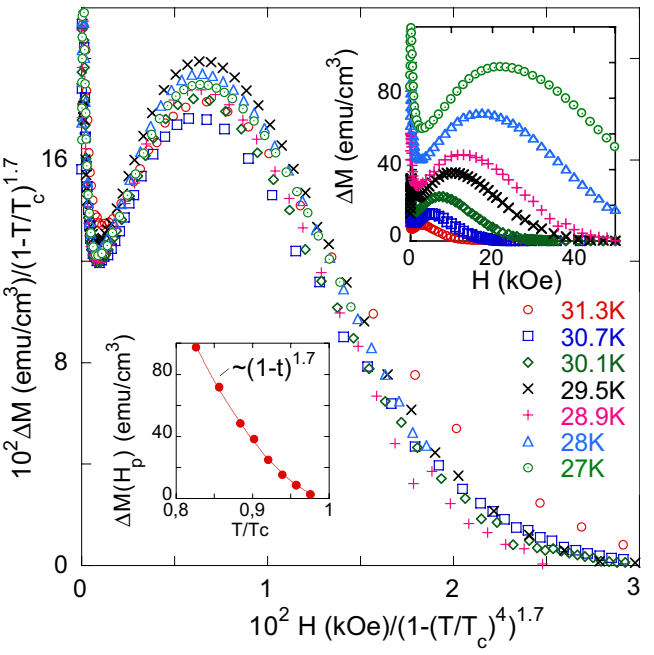

FIG. 8. (Color online) Isothermic $\Delta M/[1-(T/T_c)^4]^{1.7}$ are plotted against $H/(1-T/T_c)^{1.7}$. Upper inset shows isothermic $\Delta M(H)$ curves used in the main figure. The lower inset show a plot with values of ΔM extracted from curves in the upper inset for $H=H_p$ plotted against the reduced temperature T/T_c.

Several different approaches presented in the literature[22,28–30] allow one to obtain the activation energy $U(M)$ from $M(t)$ curves. Here, the activation energy $U(M)$ is obtained for each $M(t)$ curve by applying an approach developed by Maley *et al.*[22] where

$$U = -T\ln[dM(t)/dt] + CT$$

and C is a constant which depends on the hoping distance of the vortex, the attempt frequency and the sample size. We should mention that similar $U(M)$ curves can also be obtained from $M(t)$ curves by following an approach developed in Ref. 28. The insets of Figs. 3(a) and 3(b) show results of this approach with $C=27$ (this value will be justified below) after application to selected $M(t)$ curves obtained for fixed magnetic fields at selected temperatures. The temperatures are selected in a way that each $M(t)$ curve for a given field is located below the field H_p of its original $M(H)$ curve (but above Hon) as in Fig. 3(a) and above H_p as in Fig. 3(b). This condition is necessary since pinning mechanisms below and above H_p might be of different nature.[21] As shown in these figures, the $U(M)$ curves do not form a smooth curve with M, which is expected for temperatures very close to T_c.[31] To obtain a smooth curve we have to scale the activation-energy curves shown in the insets of Figs. 3(a) and 3(b) by a $g(T/T_c)$ scaling function.

Figures 3(a) and 3(b) show the results obtained by choosing $g(T/T_c)=(1-T/T_c)^{1.5}$. This scaling function of $U(M)$ was suggested in Ref. 31 and relies on pinning length scales for temperatures close to T_c.[32] The interesting result of Fig. 3

is that below H_p (Hon$\lesssim H\lesssim H_p$), the smooth curves follow a power law with $M^{-1.4}$ as expect from the collective pinning theory[21] but a log M behavior is obtained for fields above H_p. The above analysis yield a constant $C=27$ for our sample which is used to obtain the activation energy $U(M)$ for each $M(t)$ curve (we mention that this value of $C=27$ is of the same order as values obtained for high-T_c cuprates[31]).

Figure 4 shows a selected $M(H)$ curve measured at $T=29.5$ K. The $M(H)$ curve is plotted with magnetic relaxation data obtained over 1 h (4000 s) for fixed magnetic fields going from below Hon to above H_p. The lower inset of Fig. 4 shows details of the low-field data, providing evidence of the behavior before and after the field Hon. The upper inset show results of the relaxation rate S (right y axis) and exponent ν (left y axis) plotted as a function of H. The values of S and of the exponent ν were obtained as discussed above, by analyzing each $M(t)$ curve and the respective $U(M)$ curve. It is interesting to note that the behavior of S and ν with H is quite similar. The relaxation rate drops as field increases from below Hon up to a field close to H_p (the second peak position), increasing again as H become larger than H_p. Similar curves for S and ν as a function of H were observed on all $M(H)$ curves over which we measured magnetic relaxation.

In addition to the fact that the exponent ν follows the inverse trend of the relaxation rate S as a function of H, the absolute values of ν can provide relevant information about the pinning mechanism.[21] As shown in the upper inset of Fig. 4, the region of fields between Hon and H_p corresponds to the region where $-\nu\approx 1$ for which the relation $U(H,M)=U_{0col}(H)[M(t)/M_0]^{\nu}$ predicted by the collective pinning theory might apply. Values of $-\nu\approx 1$ are expected from collective pinning theory while values much smaller than 1, as observed on $M(t)$ curves below Hon and above H_p, may be due to single-vortex pinning regime for lower fields or plastic pinning occurring above H_p, respectively.[21]

Figures 5(a) and 5(b) show $U(M)$ curves as obtained from $M(t)$ curves appearing in Fig. 4. Figure 5(a) show a set of $U(M)$ curves for fields $H\lesssim$Hon plotted with a set of $U(M)$ for Hon$\lesssim H\lesssim H_p$. Figure 5(b) shows a set of $U(M)$ curves for fields Hon$\lesssim H\lesssim H_p$ plotted with a set of $U(M)$ curves for $H\gtrsim H_p$. It is possible to see from these plots that the fields Hon and H_p are, in fact, characteristic fields separating regions with differences in the vortex dynamics. Following the results of Ref. 21 we fit $U(M)$ for fields above H_p with the expression $U_{pl}=U_{0pl}(H)(1-\sqrt{M(t)/M_{0pl}})$. This is the appropriated description for plastic motion. Results of the fitting of $U(M)$ to the collective pinning expression of U performed for Hon$\lesssim H\lesssim H_p$ and to the plastic expression of U performed for fields $H\gtrsim H_p$ produced values of $U_{0col}(H)$ and $U_{0pl}(H)$ which show a power-law behavior with H. As expected, $U_{0col}(H)\approx H^{0.4}$ increases with field while $U_{0pl}(H)\approx H^{-0.7}$ decreases with field. The above exponents of H are used to scale the correspondents $U(H,M)$ curves shown in Figs. 5(a) and 5(b) turning them into smooth curves of $U(M)$ (in arbitrary units) plotted against $M(t)$. The results of this scaling are shown in Fig. 5(c). It is interesting to observe that each scaled curve follows a power-law behavior with M where each exponent value agrees with the averaged value of the exponent ν found in each corresponding field region as shown in the upper inset of Fig. 4. The smooth curves of Fig. 5(c) demonstrate the existence of a crossover in the pinning mechanism as field increases above Hon as well demonstrate that the second magnetization peak in the studied sample is due to a pinning crossover mechanism, as was first demonstrated in Ref. 21 for YBaCuO. The second magnetization peak occurring at H_p is formed by a crossover in the pinning mechanism, from collective to plastic pinning as the field increases.

A visual inspection of $U(M)$ curves for $H\lesssim$Hon in Fig. 5(a) suggests that these curves have the same behavior as the curves obtained for $H\gtrsim H_p$ for which it is possible to infer that a plastic pinning dominates. However, this hypothesis is inconsistent with the fact that the activation energy $U_{0pl}(H)$ [found by fitting $U(M)$ curves for $H\lesssim$Hon to the correspondent expression for plastic pinning] for $H\lesssim$Hon increases with field. On the other hand, the scaled $U(M)$ function appearing in Fig. 5(c) for $H\lesssim$Hon was obtained assuming that $U(M)$ has a power-law dependence with H of the form $\approx H^{-0.2}$, an H dependence with a negative exponent as found in the region $H\gtrsim H_p$. These contradictory facts eliminate the possibility of plastic pinning in the region below Hon, as well as eliminate the possibility of collective pinning as observed for Hon$\lesssim H\lesssim H_p$. Figure 6 show plots of the relaxation rate $S=(1/M_0)dM/d\ln t$ as obtained from magnetic relaxation data over three selected isothermal $M(H)$ curves for fields in the region of Hon. The same trend shown in Fig. 6 of S decreasing with field was observed in all $M(H)$ isothermals, which means that, in fact, the correspondent activation energy $U_0=k_BT/S$ as defined by Beasley *et al.*[25] increases with field in the region $H\lesssim$Hon. This is an interesting finding, because due to the positive inclination of $M(H)$ for $H\lesssim$Hon one would expect U_0 to decrease with field. Since above Hon, the activation energy $U_{0col}(H)$ (collective pinning region) also increases with field, the change in the pinning mechanism occurring at Hon has a different nature (probably single to collective pinning) than the pinning crossover occurring near H_p (which is collective to plastic). The formation of the peak appears then to come from the existence of a pinning crossover, probably from single to collective pinning, as Hon is crossed. This is the field region ($H\lesssim$Hon) above which the fish-tail shape takes place.

We present in Fig. 7 the vortex-phase diagram obtained from the $M(H)$ curves. An interesting finding is that the line defined by the values of $H_p(T)$ does not touch the irreversibility line but ends at some temperature below T_c. This feature is shown in the inset of Fig. 7 which shows that the anomalous second peak in the magnetization is only well defined for temperatures below 32 K. A similar behavior for the $H_p(T)$ line was observed for a deoxygenated YBaCuO crystal.[33] The crossover from collective to plastic pinning only exists below $T\lesssim 32$ K, since $M(H)$ curves obtained above this temperature do not show the second magnetization peak. It is important to mention again that both, $H_p(T)$ as well Hirr(T), are time dependent and $U(M)$ curves for fields close to both, $H_p(T)$ and Hirr(T), seem to be fitted by the plastic expression for the activation energy. To exemplify the time dependence of Hirr, values of Hirr obtained on $M(H)$ curves by using different time windows, as, for instance, show in the upper inset of Fig. 2, are plotted with values of

T_{irr} obtained from isofield M vs T curves (not shown). It is interesting to note that the values of T_{irr} are close to the values of Hirr obtained 10 min after the field was stabilized. As shown in Ref. 21, the fact that both, $H_p(T)$ and Hirr(T) are time dependent (with these values being shifted to the left with time) suggests that these fields are controlled by plastic pinning with expected temperature dependence of the form $H_p(T) \approx [1-(T/T_c)^4]^{1.4}$. This expression was obtained in Ref. 21 after considering that $U_{0pl} \approx H^{-0.7}$. Since our fittings of $U(M)$ in the region $H \gtrsim H_p$ produced a similar behavior for U_{0pl} with H, with an exponent of H varying from -0.6 to -0.7 depending on the temperature of the $M(H)$ curve, we also start our fittings of the $H_p(T)$ and Tirr(H) lines by assuming the temperature dependence $\approx [1-(T/T_c)^4]^{1.4}$. However, the best fittings, as shown in Fig. 7, were obtained with a slightly different expression, $\approx [1-(T/T_c)^4]^{1.7}$. For consistence we only fit values of Tirr(H). For the Hon(T) line we try the general expression $\approx (1-T/T_c)^m$, where m is a fitting parameter. [This expression failed to fit Hirr(T) data as well as the high-temperature region of $H_p(T)$ data]. The best fit shown in Fig. 7 was obtained with $m=1.35$. This value of the exponent m is very close to 1.5, and we observe that the value of $m=1.5$ [corresponding to the temperature dependence of the pinning length scale assumed for $g(T/T_c)$] also produced a reasonable fitting of Hon(T) data suggesting single pinning of vortices in the region below Hon. The dotted line linking the $T_c(H)$ points is only a guide to the eyes. The values of $T_c(H)$ plotted in Fig. 7 were extracted from results obtained in the same sample in Ref. 23.

We plot in Fig. 8 an attempt to scale several ΔM vs H curves which were obtained by subtracting the two branches of each respective $M(H)$ curve. The main figure shows a plot of several $\Delta M/[1-(T/T_c)^4]^{1.7}$ vs $H/(1-T/T_c)^{1.7}$ curves which reflects the consistency of the analysis performed in this work. The upper inset shows the original ΔM vs H curves. Since the H_p vs T line in Fig. 7 follows a dependence with $[1-(T/T_c)^4]^{1.7}$, we find it natural to choose the same temperature dependence to scale the x axis which is the magnetic field H. The scaling law used in the y axis, ΔM, was based on the fact that the strength of the critical current which is of the order of ΔM, should follow the temperature dependence of the pinning length scale, which for temperatures close to T_c has the form[32] $(1-T/T_c)^{1.5}$ [this is the same scaling function $g(T/T_c)$ used on the analysis of the activation energy presented in Fig. 2]. The lower inset of Fig. 8 shows a plot of ΔM for $H=H_p$ vs T/T_c, which shows a dependence with $(1-T/T_c)^{1.7}$ instead $(1-T/T_c)^{1.5}$. For this reason we choose to scale δM with $(1-T/T_c)^{1.7}$ instead $(1-T/T_c)^{1.5}$ which produced a better scaling of the curves.

IV. CONCLUSIONS

In conclusion, our study of the vortex dynamics in $Ba_{1-x}K_xFe_2As_2$ shows that the second magnetization peak occurring at H_p is formed by a crossover in the pinning mechanism, from collective to plastic pinning as the field increases. This crossover only exists below a certain temperature $T \lesssim 32$ K, since $M(H)$ curves obtained above this temperature do not show the second magnetization peak. It is also shown the existence of a pinning crossover, probably from single to collective pinning, as Hon is crossed. This is the field region ($H \lesssim$ Hon) above which the fish-tail shape takes place. Results of this work show that both $H_p(T)$ as well Hirr(T) are time dependent and their temperature dependence are well explained by an expression predicted by assuming a plastic motion of the vortex state. We also show that the $g(T/T_c)$ scaling function of $U(M)$ curves (used in Fig. 3) and the temperature-dependence expression used to fit the $H_p(T)$ and Hirr(T) lines can be used to scale several $\Delta M(H)$ producing a reasonable collapse of the curves.

ACKNOWLEDGMENTS

S.S.S., L.G., and A.D.A. thanks support from the Brazilian agencies CNPq and FAPERJ. K.M., K.Y., and L.F.C. thank the UK Funding Council EPSRC under Grant No. EP/H040048. We thank Y. Yeshurun for a helpful discussion.

[1] Y. Kamihara, T. Watanabe, M. Hirano, and H. Hosono, J. Am. Chem. Soc. **130**, 3296 (2008).
[2] M. Rotter, M. Tegel, and D. Johrendt, Phys. Rev. Lett. **101**, 107006 (2008).
[3] H. Q. Luo, Z. S. Wang, H. Yang, P. Cheng, X. Zu, and H.-H. Wen, Supercond. Sci. Technol. **21**, 125014 (2008).
[4] Y. Yeshurun and A. P. Malozemoff, Phys. Rev. Lett. **60**, 2202 (1988).
[5] Y. Yeshurun, A. P. Malozemoff, and A. Shaulov, Rev. Mod. Phys. **68**, 911 (1996).
[6] L. F. Cohen, G. Perkins, J. Laverty, W. Assmus, and A. D. Caplin, Cryogenics **33**, 352 (1993).
[7] L. F. Cohen and H. Jensen, Rep. Prog. Phys. **60**, 1581 (1997).
[8] B. Rosenstein, B. Ya. Shapiro, I. Shapiro, Y. Bruckental, A. Shaulov, and Y. Yeshurun, Phys. Rev. B **72**, 144512 (2005).
[9] B. Rosenstein and V. Zhuravlev, Phys. Rev. B **76**, 014507 (2007).
[10] G. K. Perkins, L. F. Cohen, A. A. Zhukov, and A. D. Caplin, Phys. Rev. B **51**, 8513 (1995).
[11] H. Yang, C. Ren, L. Shan, and H.-H. Wen, Phys. Rev. **78**, 092504 (2008).
[12] J. D. Moore, L. F. Cohen, Y. Yeshurun, A. D. Caplin, K. Morrison, K. A. Yates, C. M. McGilvery, J. M. Perkins, D. W. McComb, C. Trautmann, Z. A. Ren, J. Yang, W. Lu, X. L. Dong, and Z. X. Zhao, Supercond. Sci. Technol. **22**, 125023 (2009).
[13] B. Shen, P. Cheng, Z. Wang, L. Fang, C. Ren, L. Shan, and H.-H. Wen, Phys. Rev. B **81**, 014503 (2010).
[14] Y. Nakajima, T. Taen, and T. Tamegai, J. Phys. Soc. Jpn. **78**, 023702 (2009).
[15] A. Yamamoto, J. Jaroszynski, C. Tarantini, L. Balicas, J. Jiang, A. Gurevich, D. C. Larbalestier, R. Jin, A. S. Sefat, M. A. McGuire, B. C. Sales, D. K. Christen, and D. Mandrus, Appl.

Phys. Lett. **94**, 062511 (2009).
[16] R. Prozorov, N. Ni, M. A. Tanatar, V. G. Kogan, R. T. Gordon, C. Martin, E. C. Blomberg, P. Prommapan, J. Q. Yan, S. L. Bud'ko, and P. C. Canfield, Phys. Rev. B **78**, 224506 (2008).
[17] M. R. Eskildsen, L. Ya. Vinnikov, I. S. Veshchunov, T. M. Artemova, T. D. Blasius, J. M. Densmore, C. D. Dewhurst, N. Ni, A. Kreyssig, S. L. Budko, P. C. Canfield, and A. I. Goldman, Physica C **469**, 529 (2009).
[18] R. Kopeliansky, A. Shaulov, B. Ya. Shapiro, Y. Yeshurun, B. Rosenstein, J. J. Tu, L. J. Li, G. H. Cao, and Z. A. Xu, Phys. Rev. B **81**, 092504 (2010).
[19] H. Yang, H. Q. Luo, Z. S. Wang, and H.-H. Wen, Appl. Phys. Lett. **93**, 142506 (2008).
[20] J. T. Park, D. S. Inosov, Ch. Niedermayer, G. L. Sun, D. Haug, N. B. Christensen, R. Dinnebier, A. V. Boris, A. J. Drew, L. Schulz, T. Shapoval, U. Wolff, V. Neu, X. Yang, C. T. Lin, B. Keimer, and V. Hinkov, Phys. Rev. Lett. **102**, 117006 (2009).
[21] Y. Abulafia, A. Shaulov, Y. Wolfus, R. Prozorov, L. Burlachkov, Y. Yeshurun, D. Majer, E. Zeldov, H. Wuhl, V. B. Geshkenbein, and V. M. Vinokur, Phys. Rev. Lett. **77**, 1596 (1996).
[22] M. P. Maley, J. O. Willis, H. Lessure, and M. E. McHenry, Phys. Rev. B **42**, 2639 (1990).
[23] S. Salem-Sugui, Jr., L. Ghivelder, A. D. Alvarenga, J. L. Pimentel, Jr., H. Luo, Z. Wang, and H.-H. Wen, Phys. Rev. B **80**, 014518 (2009).
[24] G. K. Perkins, J. Moore, Y. Bugoslavsky, L. F. Cohen, J. Jun, S. M. Kazakov, J. Karpinski, and A. D. Caplin, Supercond. Sci. Technol. **15**, 1156 (2002).
[25] M. R. Beasley, R. Labash, and W. W. Weeb, Phys. Rev. **181**, 682 (1969).
[26] D. Shi and S. Salem-Sugui, Jr., Phys. Rev. B **44**, 7647 (1991).
[27] S. Salem-Sugui, Jr., A. D. Alvarenga, M. Friesen, K. C. Goretta, O. F. Schilling, F. G. Gandra, B. W. Veal, and P. Paulikas, Phys. Rev. B **71**, 024503 (2005).
[28] S. Sengupta, D. Shi, S. Salem-Sugui, Jr., Z. Wang, P. J. McGinn, and K. DeMoranville, J. Appl. Phys. **72**, 592 (1992).
[29] R. Griessen, Wen Hai-hu, A. J. J. van Dalen, B. Dam, J. Rector, H. G. Schnack, S. Libbrecht, E. Osquiguil, and Y. Bruynseraede, Phys. Rev. Lett. **72**, 1910 (1994).
[30] H. H. Wen, H. G. Schnack, R. Griessen, B. Dam, and J. Rector, Physica C **241**, 353 (1995).
[31] M. E. McHenry, S. Simizu, H. Lessure, M. P. Maley, J. Y. Coulter, I. Tanaka, and H. Kojima, Phys. Rev. B **44**, 7614 (1991).
[32] M. Tinkham, Phys. Rev. Lett. **61**, 1658 (1988).
[33] S. Salem-Sugui, Jr., L. Ghivelder, M. Friesen, K. Moloni, B. Veal, and P. Paulikas, Phys. Rev. B **60**, 102 (1999).